SUPPLEMENTAL MATERIAL

Lee et al., https://doi.org/10.1084/jem.20170690

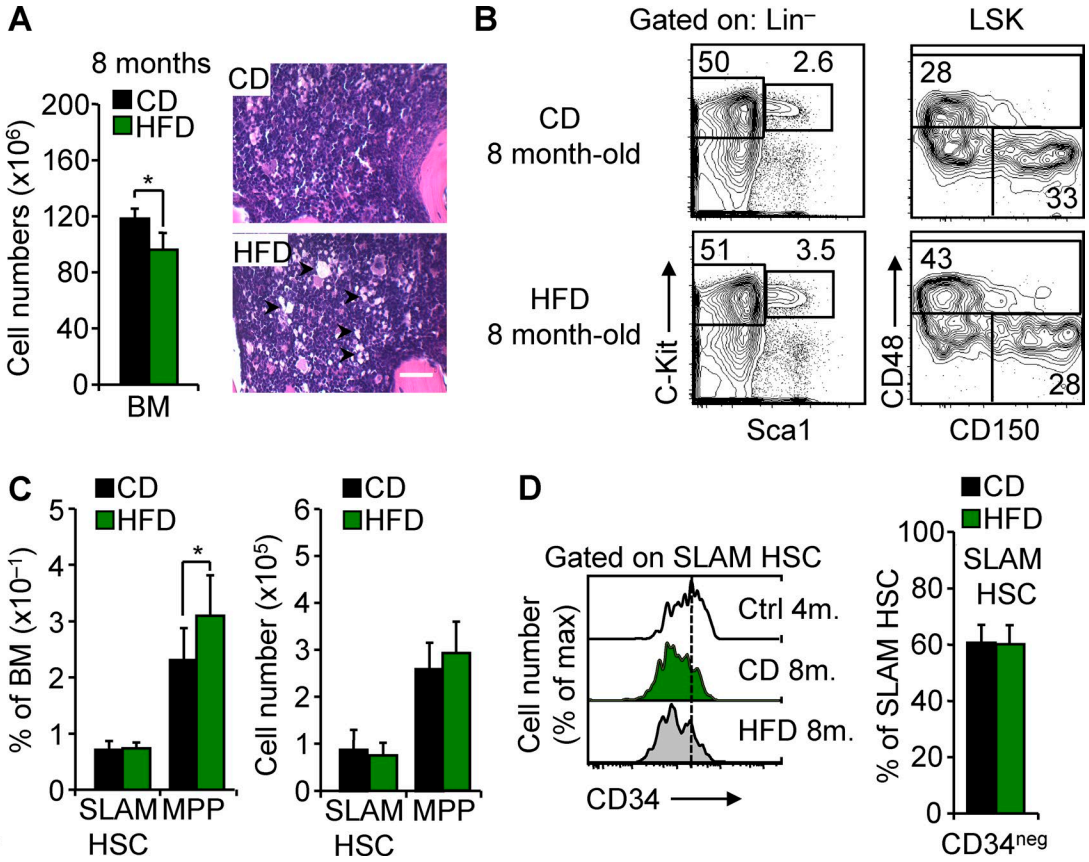

Figure S1. **Hematopoietic disruption in obesity. (A)** BM cellularity of 8-mo-old HFD-fed mice compared with CD-fed littermates. Results are expressed as means ± SD. *n* = 9/group. Images show H&E staining of BM sections from CD and HFD mice (*n* = 3). Arrowheads indicate adipocytes. Bar, 100 µm. **(B)** FACS plots of HSPC populations in the BM 8-mo-old CD and HFD mice. *n* = 9. **(C)** Mean percentages ± SD (left) and absolute numbers (right) of HSPC populations in the BM of 4-mo-old *Ctrl* and *db* mice. *n* = 9/group. Student's *t* test; *, P ≤ 0.05. **(D)** Representative FACS plots showing expression of the CD34 marker in SLAM HSCs (left) and mean percentages ± SD (right) of HFD SLAM HSCs negative for CD34. *n* = 9/group.

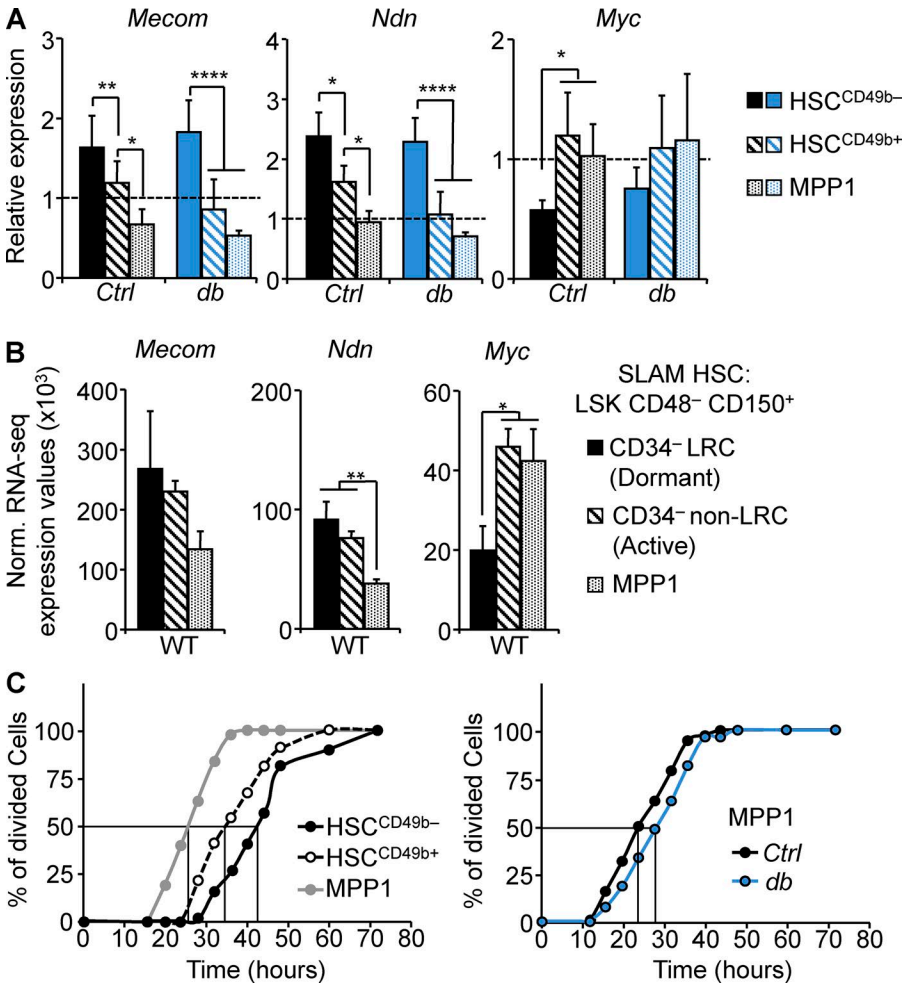

Figure S2. **Molecular characteristics of the HSC subsets isolated from *Ctrl* and *db* mice. (A)** qRT-PCR analyses for *Mecom*, *Myc*, and *Ndn* gene expression in HSC subsets isolated from 4-mo-old *Ctrl* and *db* mice. Results are expressed as fold change ± SD relative to total *Ctrl* SLAM HSCs set at 1. $n = 6$ pools of 100 cells. Two-way ANOVA with Tukey's post hoc test; *, $P \leq 0.05$; **, $P \leq 0.005$; ****, $P \leq 0.0001$. Two independent experiments. **(B)** Mean RNA-seq expression for *Mecom*, *Myc*, and *Ndn* transcripts in dormant LRC HSCs, active non-LRC HSCs, and MPP1 cells. $n = 3$ pools/group. One-way ANOVA with Tukey's post hoc test; *, $P \leq 0.05$; **, $P \leq 0.005$ (Cabezas-Wallscheid et al., 2017). **(C)** Single-cell tracking measuring the kinetics of the first division for cultured HSC subsets. Results are expressed as percentages of cells able to divide at least once during 72 h culture. The left panel shows the cell division kinetics of HSC subsets isolated from WT mice ($n = 20$, 30, and 43 cells, respectively). The right panel shows the cell division kinetics for MPP1 cells isolated from 4-mo-old *Ctrl* and *db* mice ($n = 38$ and 29 cells, respectively). Data are representative of two independent experiments.

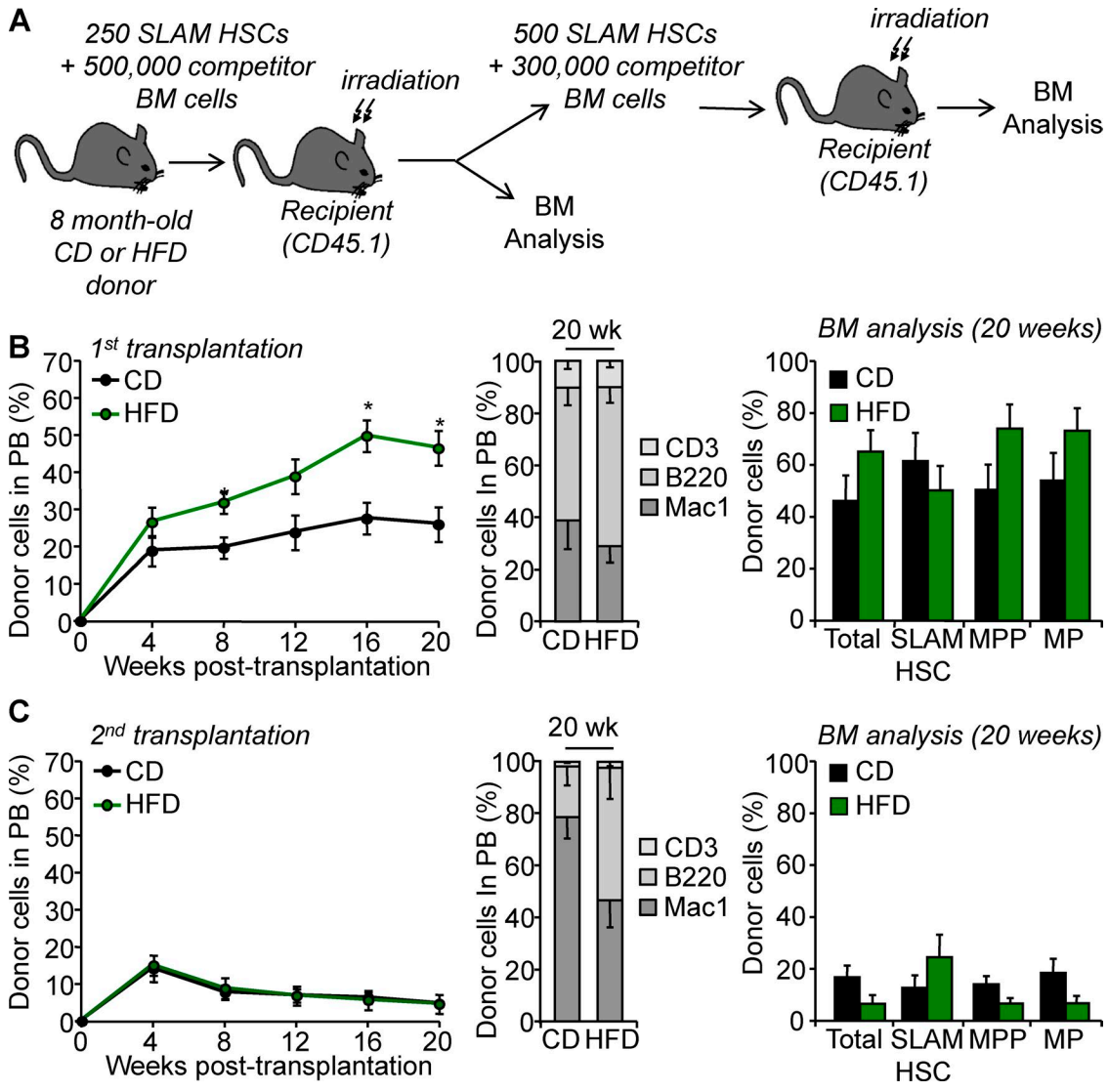

Figure S3. **Validation of the HSC functional dysregulation in dietary mouse model. (A)** Experimental scheme for serial transplantation assay. **(B and C)** Hematopoietic reconstitution in primary and secondary recipients. The left graph indicates PB chimerism over time. The middle graph shows myeloid and lymphoid PB chimerism 20 wk after transplantation. The right graph shows the percentage of donor-derived total BM cells, SLAM HSCs, MPPs, and myeloid progenitors (MPs) 20 wk after transplantation. Results are expressed as means ± SEM. n = 4/group. Student's t test; *, $P \leq 0.05$. Two independent experiments.

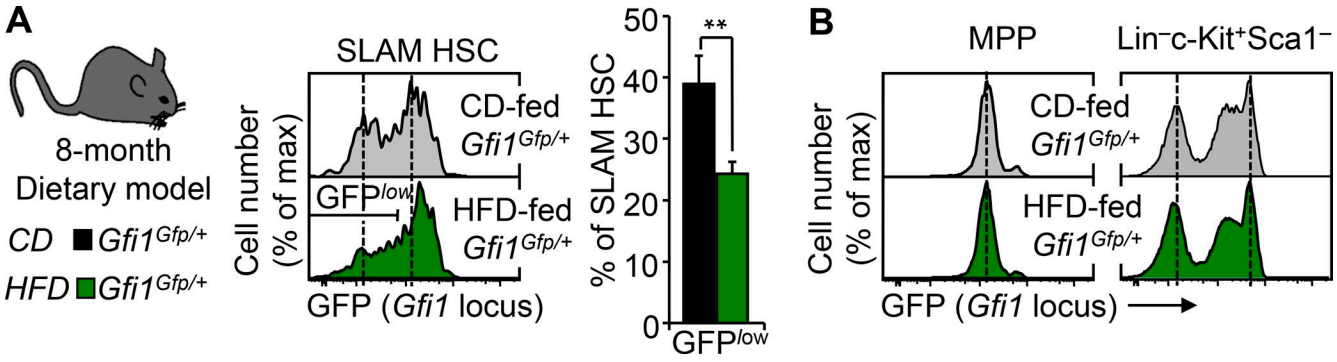

Figure S4. **Activity of the *Gfi1* locus in HSCs isolated from mice fed with HFD. (A)** Representative FACS plots showing GFP fluorescence in the SLAM HSCs of 8-mo-old CD- and HFD-fed *Gfi1*$^{Gfp/+}$ mice. The graph indicates mean percentages ± SD of GFP^{low} SLAM HSCs in each condition. **, P ≤ 0.005. **(B)** Representative FACS plots showing GFP fluorescence in MPPs (left) and in LK progenitors (right) of 8-mo-old CD- and HFD-fed *Gfi1*$^{Gfp/+}$ mice. *n* = 4 mice/group.

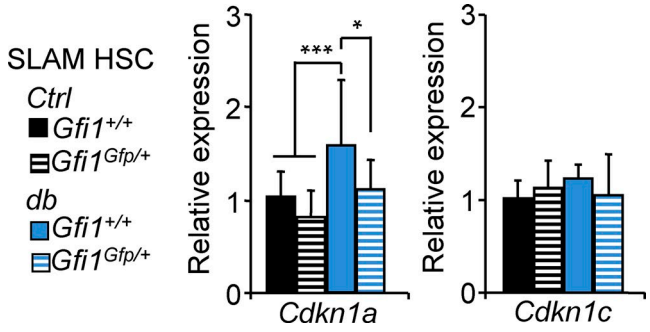

Figure S5. **Impact of *Gfi1* gene dosage on *Cdkn1a* expression.** qRT-PCR analyses for *Cdkn1a* and *Cdkn1c* genes in SLAM HSCs isolated from 4-mo-old *db*, *Ctrl::Gfi1*$^{Gfp/+}$, and *db::Gfi1*$^{Gfp/+}$ mice. Results are expressed as fold change ± SD relative to control SLAM HSCs. *n* = 8–18. One-way ANOVA with Tukey's post hoc test; *, P ≤ 0.05; ***, P ≤ 0.001. Two independent experiments.

Table S1. **List of antibodies used in this study**

Name	Alternative name	Clone	Fluorochrome	Source	Catalog number
Ter119	Ly-76	TER-119	Purified	BioLegend	116202
Mac1	CD11b, Integrin a	M1/70	Purified	BioLegend	101202
Gr1	Ly-6C	RB6-8C5	Purified	BioLegend	108402
B220	CD45R	RA-3-6B2	Purified	BioLegend	103202
CD5		53-7.3	Purified	BioLegend	100602
CD3		17A2	Purified	BioLegend	100202
CD4		GK1.5	Purified	BioLegend	100402
CD8		53-6.7	Purified	BioLegend	100702
CD127	IL-7Ra	A7R34	Purified	eBioscience	14-1271-85
Goat anti–rat			Pecy5	Thermo Fisher Scientific	A10691
c-kit	CD117	2B8	APC-eFluor780	eBioscience	47-1171-82
Sca1	Ly-6a/e	D7	PB	BioLegend	108120
Flk2		A2F10	Biotin	eBioscience	13-1351-85
CD48		HM48-1	A647	BioLegend	103416
CD150		TC15-12F12.2	PE	BioLegend	115904
CD34		RAM34	FITC	eBioscience	11-0341-85
FcgR		93	PerCP-eFluor710	eBioscience	46-0161-80
CD49b		DX5	Biotin	BioLegend	108903
CD49b		DX5	PerCP-Cy5.5	BioLegend	108915
Streptavidin			Pecy7	BioLegend	405206
IgM		II/41	APC-eFluor780	eBioscience	47-5790-82
B220		RA3-6B2	BV421	BioLegend	103239
CD19		eBio1D3	Alexa Fluor 700	eBioscience	56-0193-80
CD127	IL-7Ra	SB/199	Biotin	BioLegend	121104
Ki67		16A8	PE	BioLegend	652404

Table S2. **List of primers used in this study**

Primer	Direction	Sequence (5′–3′)
Gfi1	Forward	CCCGGCCCTATCCCTGTC
Gfi1	Reverse	CACCTGGCATTTGTGGGGCT
Bmi1	Forward	GGAGTAAAATGGACATACCC
Bmi1	Reverse	AAAGGTTCCTCTTCATACATG
HoxB4	Forward	CGTCTACCCCTGGATGCGC
HoxB4	Reverse	CCTGCTGGCGAGTGTAGGC
Cdkn1a	Forward	GGCGCAGATCCACAGCGAT
Cdkn1a	Reverse	GGGACCGAAGAGACAACGGC
Cdkn1b	Forward	GGGATGAGGAAGCGACCTGC
Cdkn1b	Reverse	GTGCCAGCGTTCGGGGAA
Cdkn1c	Forward	ACCAGCCTCTCTCGGGGATT
Cdkn1c	Reverse	GCAGTTCTCTTGCGCTTGGC
Myc	Forward	AGGCTGGATTTCCTTTGGGCGTT
Myc	Reverse	GTTGAGGGGCATCGTCGTGG
Mecom	Forward	TGTGCCAGAGGAGCTTAAACAGACG
Mecom	Reverse	GGGAGGTGGGATGGAGGGAAT
Ndn	Forward	GCTCATGTGGTACGTGTTGG
Ndn	Reverse	TGCTTCTGCACCATTTCTTG
Actb	Forward	CCCTAAGGCCAACCGTGAAA
Actb	Reverse	CAGCCTGGATGGCTACGTAC

Table S3 is a separate Excel document showing source data for the heatmap of bulk gene expression and GSEAs generated from 4-mo *Ctrl* and *db* SLAM HSCs.

REFERENCE

Cabezas-Wallscheid, N., F. Buettner, P. Sommerkamp, D. Klimmeck, L. Ladel, F.B. Thalheimer, D. Pastor-Flores, L.P. Roma, S. Renders, P. Zeisberger, et al. 2017. Vitamin A-Retinoic Acid Signaling Regulates Hematopoietic Stem Cell Dormancy. *Cell*. 169:807–823. https://doi.org/10.1016/j.cell.2017.04.018